UBC13-mediated template switching promotes replication stress resistance in FBH1-deficient cells

Alexandra L. Hawks[1#], Amy Bergmann[1#], Tyler J. McCraw[1], and Jennifer M. Mason[1*]

[1]Department of Genetics and Biochemistry, Clemson University, Clemson University

# Equal contribution

Keywords: FBH1, replication stress, template switching, UBC13, RAD51

*To whom correspondence should be addressed:

Jennifer M. Mason, Ph.D.
Department of Genetics and Biochemistry
Clemson University
130 McGinty Court
154 Poole
Clemson, SC 29634
Email address: jmason4@clemson.edu

ABSTRACT

The proper resolution of DNA damage during replication is essential for genome stability. FBH1, a UvrD, helicase plays crucial roles in the DNA damage response. FBH1 promotes double strand break formation and signaling in response to prolonged replication stress to initiate apoptosis. Human FBH1 regulates RAD51 to inhibit homologous recombination. A previous study suggested that mis-regulation of RAD51 may contribute to replication stress resistance in FBH1-deficient cells, but the underlying mechanism remains unknown. Here, we provide direct evidence that RAD51 promotes replication stress resistance in FBH1-deficient cells. We demonstrate inhibition of RAD51 using the small molecule, B02, partially rescues double strand break signaling in FBH1-deficient cells. We show that inhibition of only the strand exchange activity of RAD51 rescues double strand break signaling in FBH1 knockout cells. Finally, we show that depletion of UBC13, a E2 protein that promotes RAD51-dependent template switching, rescues double strand break formation and signaling sensitizing FBH1-deficient cells to replication stress. Our results suggest FBH1 regulates template switching to promote replication stress sensitivity.

INTRODUCTION

DNA must be accurately replicated each cell cycle to maintain the integrity of the genome. Replication stress caused by depletion of nucleotide pools, collision between replication and transcription machinery, or DNA damage slows and/or stalls replication forks threatening genome stability[1]. In response to replication stress, cells activate the DNA damage response that includes cell cycle checkpoints and DNA repair pathways. Defects in the replication stress response increase genome instability and contribute to human disease such as cancer[2,3].

Upon replication fork stalling, fork regression occurs by re-annealing nascent DNA strands to convert a replication fork from a 3-way junction to a 4-way junction[4]. There are multiple proteins that mediate fork regression in cells and function in at least two independent pathways. HLTF, SMARCAL1, and ZRANB3 function in one pathway, and FBH1 functions in the second pathway[5–11]. RAD51 is required for fork regression in both the HLTF- and FBH1-dependent pathways[12,13]. RAD51 is stabilized on the regressed arm to protect the newly synthesized DNA from degradation by nucleases including MRE11[14,15]. Therefore, fork regression is proposed to maintain genome integrity by preventing nucleolytic degradation of replication forks.

Other DNA damage tolerance pathways including translesion synthesis (TLS), PRIMPOL-mediated repriming, and template switching function in the response to replication stress. Emerging evidence indicates fork regression also limits replication progression in response to stresses by inhibiting TLS and PRIMPOL-mediated repriming. TLS polymerases such as Polη and Polκ are recruited to stalled replication forks after proliferating cell nuclear antigen (PCNA) mono-ubiquitination at lysine-164 by RAD18[16]. TLS polymerases can bypass lesions allowing replication to continue even in the presence of damage. PRIMPOL uses primase

activity to reprime downstream of the replication fork and performs DNA synthesis for a few nucleotides[17]. PRIMPOL is then dissociated from the DNA to allow the replicative polymerases to continue DNA synthesis. PRIMPOL can be used to bypass UV lesions and bulky lesions to complete DNA replication[17,18]. Fork regression mediated by HLTF, RAD51, and SMARCAL1 prevents PRIMPOL-mediated repriming at stalled replication forks[10,19–21]. Increased PRIMPOL activity contributes to cisplatin resistance in BRCA1-deficient cells[19]. In addition to TLS and PRIMPOL-mediated repriming, template switching functions at replication forks. RAD51-dependent template switching uses the complementary sister chromatid to extend the nascent ssDNA resulting in lesion bypass[22]. PCNA polyubiquitination at lysine-164 by UBC13, MMS2 and HLTF/SHPRH promotes template switching[23–26]. The ssDNA gaps left by PRIMPOL are repaired by post-replication repair pathways including TLS during S and G2 phase or template switching during S phase[21].

These studies demonstrate that fork reversal plays an important role in regulating TLS and PRIMPOL-mediated repriming, but we do not fully understand how template switching is regulated at stalled replication forks in human cells. In *S. cerevisiae*, SUMOylation of PCNA inhibits homologous recombination (HR) in S phase by recruiting the anti-recombinase Srs2 resulting in disassembly of Rad51 presynaptic filaments[27–30]. In *S. pombe,* Srs2 and Fbh1 suppress Rad51-mediated homologous recombination at stalled replication forks inhibiting template switching-dependent replication restart[31–33]. However, human FBH1 inhibition of template switching at stalled replication forks has not been thoroughly addressed.

FBH1 is a UvrD helicase with 3'-5' activity that functions in response to replication stress[34,35]. FBH1 promotes MUS81-dependent cleavage of stalled replication forks in response to prolonged treatment with hydroxyurea (HU) and ultra-violet (UV) radiation[36,37]. Hemizygous or

48 homozygous loss of FBH1 was found in up to 63% of cell lines derived from metastatic
49 melanoma[38]. Furthermore, FBH1 protects melanocytes from UV-mediated malignant
50 transformation suggesting FBH1 plays an important role in preventing tumorigenesis. However,
51 how FBH1 promotes MUS81-dependent cleavage of stalled replication forks is not clear.
52 To date, there have been two proposed mechanisms for how FBH1 promotes double
53 strand break (DSB) formation and cell death in response to prolonged replication stress. First,
54 FBH1 mediates fork regression in response to HU[8]. In this instance, the absence of fork
55 regression can lead to increased PRIMPOL-mediated repriming or TLS as seen in HLTF-
56 deficient cells[10]. Second, FBH1 is unique among the fork remodeling enzymes because FBH1
57 inhibits HR by disassembling RAD51 presynaptic filaments from ssDNA[39–42]. FBH1 contains an
58 FBOX that interacts with SKP1 to form a SKP1-CUL1-FBOX (SCF) protein complex that
59 functions as an E3 ubiquitin ligase[34,35]. After FBH1 removes RAD51 from ssDNA, the SCF^{FBH1}
60 ubiquitinates RAD51 to prevent reassociation of RAD51 with DNA[34,35,40]. Expression of a
61 ubiquitination-resistant mutant of RAD51, RAD51 K58/64R, results in reduced DSB formation
62 and increased survival in response to HU, suggesting that the ability of FBH1 to regulate RAD51
63 may be important for promoting sensitivity to replication stress[42]. Whether RAD51 is
64 contributing to resistance in FBH1-deficient cells has not been directly tested.
65 In this study, we aimed to elucidate whether RAD51 plays a role in promoting resistance
66 to replication stress in FBH1-deficient cells. We demonstrated inhibition of RAD51 restores
67 DSB signaling in FBH1-deficient cells after prolonged exposure to HU. Specifically, inhibition
68 of the strand exchange of RAD51 (i.e., HR) rescued DSB signaling in FBH1-deficient cells,
69 Finally, we determined that knockdown of UBC13, a protein that promotes template switching,
70 rescued DSB signaling and sensitized FBH1-deficient cells to replication stress. Together, our

71 data suggests that FBH1 regulates template switching to promote replication stress sensitivity
72 and that inhibition of template switching may be a potential sta
73
74 **RESULTS**
75 **Inhibition of RAD51 partially restored double strand break signaling in FBH1-deficient**
76 **cells**
77 Expression of RAD51-K58/64R, a mutant that is resistant to ubiquitylation by FBH1,
78 results in increased HR activity, reduced DSB formation, and increased survival following
79 replication stress suggesting that mis-regulation of RAD51 is contributing to replication stress
80 resistance in FBH1-defcient cells[42]. We aimed to determine how RAD51 is contributing to
81 replication stress resistance in FBH1-deficient cells by testing the impact of RAD51 inhibition
82 on the cellular response to HU in FBH1-deficient cells. To do this, we knocked out FBH1 in
83 U2OS cells (hereafter FBH1 KO) and verified loss of FBH1 by western blotting (**Supplemental**
84 **Figure 1A**).
85 First, we treated U2OS and FBH1 KO cells with 2 mM HU for 24 hours with or without
86 the RAD51 inhibitor, B02, which inhibits the DNA binding activity of RAD51 and examined
87 induction of the replication stress response[43]. When replication forks stall, RPA bound to
88 ssDNA at stalled forks is phosphorylated at serine-33 (pRPA S33) by the ATR kinase[44]. We
89 quantified pRPA S33 in RPA positive cells following treatment with HU and B02 in U2OS cells.
90 We found no significant difference in the percentage of pRPA S33 positive cells between U2OS
91 and FBH1 KO cells (**Figure 1A**). The addition of B02 caused no significant change in the
92 percentage of pRPA S33 positive cells in U2OS or FBH1 KO cells. This result indicates

93 treatment with B02 does not significantly alter the replication stress response in U2OS and FBH1
94 KO cells.

95 Next, we determined if inhibition of RAD51 with B02 restored double strand break
96 signaling in FBH1-deficient cells after HU treatment. Prolonged replication stress after HU
97 treatment results in excessive ssDNA accumulation, ultimately exhausting the cellular pool of
98 RPA[45]. The exposed ssDNA is susceptible to cleavage by nucleases including MUS81[46]. After
99 end resection, RPA binds to the ssDNA overhangs and is phosphorylated at serines 4 and 8
100 (pRPA S4/8) by DNAPkcs and can be quantified using fluorescence microscopy[47]. After HU
101 treatment, 63% of RPA positive U2OS cells were pRPA S4/8 positive and B02 treatment results
102 in a small, but significant increase in pRPA S4/8 positive cells (**Figure 1B**). As reported
103 previously, FBH1-deficient cells exhibited a 2.4-fold reduction in pRPA S4/8 positive cells
104 compared to U2OS cells consistent with a defect in DSB signaling after HU treatment[36,37].
105 Treatment of FBH1 KO cells with 10 and 25 μM B02 significantly increased pRPA S4/8 positive
106 cells to 46% and 48%, respectively compared to FBH1 KO cells (**Figure 1B)**. This result
107 suggests inhibition of RAD51 partially restored DSB signaling in FBH1-deficient cells.

108 In response to DNA damage, the histone variant, H2AX, is phosphorylated at serine-
109 139[48]. Intensive, uniform γ-H2AX staining (i.e., pan-nuclear γ-H2AX) has been associated with
110 replication catastrophe[45]. Previous studies have shown FBH1-deficient cells exhibit a significant
111 reduction in pan-nuclear γ-H2AX following prolonged replication stress[36,37]. We determined if
112 B02 treatment restored induction of pan-nuclear γ-H2AX after treatment with 2 mM HU. Cells
113 were co-stained with PCNA to identify cells in S phase at the time of HU treatment. In U2OS
114 cells, 32% of PCNA positive U2OS cells were positive for pan-nuclear γ-H2AX staining and
115 B02 treatment did not significantly change the percentage of cells containing pan-nuclear γ-

116 H2AX. As expected, FBH1 KO cells had a 5-fold reduction in the percentage of cells with pan-
117 nuclear γ-H2AX staining compared to U2OS cells (7% compared to 32%) (**Figure 1C**). FBH1
118 KO cells treated with 10 and 25 μM B02 and 2 mM HU had 19% and 31% pan-nuclear γ-H2AX
119 positive cells, respectively. These data suggest that inhibition of RAD51 partially restores DNA
120 damage signaling in FBH1-deficient cells after HU treatment.
121
122 **Inhibition of the strand exchange activity of RAD51 rescues DSB signaling in FBH1 KO**
123 **cells**
124 We reasoned there are at least two potential mechanisms by which RAD51 inhibition
125 could restore DSB signaling in FBH1-deficient cells. First, RAD51 nucleoprotein filaments can
126 inhibit MUS81 cleavage[49,50]. FBH1 may be removing RAD51 from DNA to allow MUS81 to
127 access stalled forks. We hypothesized if RAD51 bound to DNA was preventing MUS81
128 cleavage, inhibition of RAD51 strand exchange (e.g. HR) would not restore DSB signaling in
129 FBH1-deficient cells. Second, similar to yeast Fbh1, human FBH1 may be inhibiting HR at
130 stalled replication forks[27–30] and would require the strand exchange of RAD51. To distinguish
131 between these two mechanisms, we treated cells with the inhibitor, RI(dl)2, that inhibits the
132 strand exchange activity of RAD51. During HR, RAD51 forms a nucleoprotein filament on
133 ssDNA using site I and performs homology search and strand exchange using site II binding site.
134 In yeast and humans, mutations in site II result in a RAD51 mutant capable of forming
135 presynaptic filaments, but deficient in carrying out recombination[13,51]. The small molecule,
136 RI(dl)2, mimics a site II mutant by inhibiting the strand exchange of RAD51 without disrupting
137 RAD51 nucleoprotein filament formation[52].

138 To determine if inhibition of HR restored DSB signaling in FBH1 KO cells, we treated
139 cells with 2 mM HU for 24 hours with or without the inhibitor, RI(dl)2, and examined induction
140 of pRPA S33. We observed no significant change in pRPA S33 staining in U2OS or FBH1 KO
141 cells with either 25 or 50 μM RI(dl)2 (**Figure 2A**). This suggests that the inhibition of the strand
142 exchange activity of RAD51 does not have a significant impact on induction of the replication
143 stress response in U2OS and FBH1 KO cells.
144 Next, we determined whether inhibition of the strand exchange activity of RAD51 had
145 any impact on DSB signaling in FBH1-deficient cells. U2OS and FBH1 KO cells were treated
146 with 2 mM HU with or without RI(dl)2 for 24 hours. In U2OS cells, 66% of RPA positive cells
147 were positive for pRPA S4/8 (**Figure 2B).** Treating U2OS cells with RI(dl)2 did not significantly
148 change the percent of RPA positive cells with pRPA 4/8 signaling, indicating RI(dl)2 treatment
149 alone is not impacting induction of DSB signaling. FBH1 KO cells had a 2-fold decrease in
150 pRPA S4/8 positive cells compared to U2OS. Treating FBH1 KO cells with 25 μM RI(dl)2
151 significantly increased pRPA S4/8 positive cells to 61% compared to the FBH1 KO. When
152 treated with 50μM RI(dl)2, FBH1 KO cells exhibited induction of pRPA S4/8 similar to U2OS
153 cells with 72% of RPA positive cells containing pRPA S4/8. This result suggests that inhibition
154 of strand exchange activity of RAD51 restores DSB signaling in FBH1-deficient cells after HU
155 treatment.
156
157 **UBC13 knockdown restores DSB signaling in FBH1-deficient cells**
158 As inhibition of the strand exchange activity of RAD51 restored DSB signaling, we next
159 asked if inhibition of template switching, a DDT pathway that requires the strand exchange
160 activity of RAD51 at stalled replication forks, restored DSB signaling in FBH1-deficient cells[53].

161 The E2 protein, UBC13, works with SHRPH to contribute to polyubiquitination of PCNA at
162 lysine 164 to promote RAD51-dependent template switching[23,54]. We depleted UBC13 from
163 U2OS and FBH1 KO cells using siRNAs (**Supplemental Figure 1B**). Cells were then treated for
164 24 hours with 2 mM HU and stained for the DSB marker pRPA S4/8. U2OS cells had
165 approximately 70% of RPA positive cells that were also positive for pRPA S4/8 and knockdown
166 of UBC13 did not result in a significant difference in the percentage of pRPA S4/8 cells (**Figure**
167 **3A**). In FBH1 KO cells, we observed a 2-fold decrease in pRPA S4/8 positive cells compared to
168 the non-silencing control in U2OS (siNS). When UBC13 was knocked down in FBH1 KO cells,
169 we observed a significant increase in the percentage of pRPA S4/8 cells from 37% to 69%. We
170 observed a similar result when we examined pan-nuclear γ–H2AX in U2OS and FBH1 KO upon
171 UBC13 knockdown (**Figure 3B**). Compared to U2OS, FBH1 KO cells exhibited a 4-fold
172 decrease in pan-nuclear γ–H2AX positive cells. When UBC13 was depleted in FBH1 KO cells,
173 the percentage of pan-nuclear γ–H2AX positive cells increased from 9% to 28% indicating
174 depletion of UBC13 rescues DSB signaling defect in FBH1-deficient cells.
175 Next, we determined if depletion of UBC13 would rescue DSB signaling in siFBH1
176 transfected RPE-1 cells. RPE-1 cells transfected with the non-silencing control (siNS) contained
177 66% RPA positive cells that were also pRPA S4/8 positive and knockdown of UBC13 alone
178 (siUBC13) did not significantly change the percentage of pRPA S4/8 cells (**Supplemental**
179 **Figure 2A**). Like U2OS cells, FBH1-depleted cells (siFBH1) exhibited a significant reduction in
180 pRPA S4/8 positive cells (24%) and knocking down UBC13 increased pRPA positive cells to
181 53%. We observed a similar result when we examined pan-nuclear γ–H2AX in RPE-1 cells
182 (**Supplemental Figure 2B**). Cells transfected with siNS exhibited 34% of γ–H2AX positive cells
183 and UBC13 knockdown did not significantly change the percentage of cells containing pan-

184 nuclear γ–H2AX. Knockdown of FBH1 reduced the percentage of cells with pan-nuclear
185 γ–H2AX to 6% and knockdown of UBC13 rescued induction of pan-nuclear γ–H2AX (34%).
186 Together, these results indicated depletion of UBC13 rescues DSB signaling in FBH1-deficient
187 cells.
188
189 **UBC13 knockdown rescues DSB formation in FBH1-deficient cells**
190 FBH1 works with MUS81 to promote DSB formation in response to prolonged
191 replication stress[36]. FBH1-deficient cells exhibit a significant reduction in DSBs after prolonged
192 HU treatment. To determine if depletion of UBC13 rescues DSB formation in FBH1-deficient
193 cells, U2OS and FBH1 KO cells were treated for 24 hours with 2 mM HU and DSBs were
194 detected using the TUNEL assay that has been previously shown to detect excessive breakage
195 due to replication catastrophe[45]. After HU treatment, depletion of UBC13 in U2OS cells resulted
196 in a slight decrease in TUNEL positive cells from 32% to 27% (**Figure 4A**). In FBH1 KO cells,
197 we observed a significant decrease in TUNEL positive cells (1%) compared to U2OS cells.
198 When we depleted UBC13 in FBH1 KO cells, the TUNEL positive cells increased to 25%. A
199 similar result was observed in RPE-1 cells depleted of UBC13 and FBH1 (**Figure 4B**).
200 Compared to siNS-transfected cells, FBH1-depleted cells exhibited a 17-fold reduction in
201 TUNEL positive cells. Depletion of UBC13 in siFBH1-transfected cells increased the
202 percentage of TUNEL positive cells from 2% to 26%. Taken together, these results indicate that
203 inhibition of UBC13 restores DSB formation and signaling in FBH1-deficient cells treated with
204 HU.
205
206 **UBC13 sensitizes FBH1-deficient cells to HU**

207 In FBH1-deficient cells, reduced DSB break formation results in increased resistance to
208 HU[36,37]. Given UBC13 depletion restored DSB formation and signaling in FBH1-deficient cells,
209 we next determined if UBC13 depletion restored sensitivity of FBH1-deficient cells to HU. We
210 treated cells with increasing amounts of HU and measured cell survival. As expected, FBH1 KO
211 cells had increased survival compared to U2OS consistent with FBH1 KO cells being resistant to
212 replication stress (**Figure 5**). Depletion of UBC13 in U2OS cells had no significant impact on
213 cell survival in response to HU. Importantly, when UBC13 was knocked down in FBH1 KO
214 cells, there was a significant decrease in survival compared to the FBH1 KO cells. Together,
215 these data suggest that inhibition of UBC13 sensitizes FBH1-deficient cells to replication stress
216 by restoring DSB formation.
217
218 **DISCUSSION**
219 FBH1 is an anti-recombinase that inhibits HR by removing RAD51 from ssDNA at
220 stalled replication forks[39–41]. As part of the SCF^{FBH1} complex, FBH1 mediates the ubiquitination
221 of RAD51 to prevent reassociation with DNA[34,35,40]. Over-expression of a ubiquitination
222 resistant RAD51 mutant resulted in decreased DSB formation and increased resistance to HU
223 suggesting regulation of RAD51 by FBH1 is important to promote sensitivity to replication
224 stress[41]. However, it is not known if K58/K64R disrupted functions of RAD51 as the
225 biochemical activities of RAD51 K58/K64R were not tested. Here, we provide direct evidence
226 that inhibition of RAD51 filament assembly or strand exchange restores DSB signaling in FBH1-
227 deficient cells after HU treatment. In addition, we demonstrate depletion of UBC13 restores DSB
228 signaling and sensitizes FBH1-deficient cells to replication stress. Together, these results
229 indicate loss of template switching restores replication stress sensitivity in FBH1-deficient cells.

230 RAD51 nucleoprotein filaments bound to stalled replication forks can inhibit MUS81
231 access to DNA preventing DSB formation[49,50]. The anti-recombinases yeast Srs2 and human
232 RECQ5 have been shown to remove RAD51 from DNA to promote MUS81 cleavage. Thus, one
233 possibility is that FBH1 removes RAD51 from stalled replication forks to promote MUS81-
234 dependent DSB formation. Consistent with this model, inhibition of RAD51 filament assembly
235 resulted in partial rescue of DSB signaling after prolonged HU treatment in FBH1 KO cells. We
236 predicted that if this was the primary mechanism of replication stress resistance in FBH1-
237 deficient cells, inhibition of strand exchange activity of RAD51 without disruption of RAD51
238 nucleofilament assembly would not restore DSB signaling. However, our data suggest that
239 inhibiting the strand exchange activity of RAD51 or depleting UBC13 restores levels of DSBs
240 signaling and sensitivity in FBH1-deficient cells to levels observed in U2OS cells indicating the
241 primary mechanism underlying replication stress resistance in FBH1-deficient cells involves HR.
242 UBC13 is an ubiquitin E2 conjugating enzyme that forms polyubiquitin chains with
243 different E3 enzymes in multiple cellular pathways including TRAF-mediated inflammatory
244 response, DSB repair and template switching[55–58]. UBC13 polyubiquitinates PCNA to promote
245 RAD51-dependent template switching[55]. Our results indicate that depletion of UBC13 sensitizes
246 FBH1 KO cells to HU. Given inhibition of the strand exchange of RAD51 also restores DSB
247 signaling in FBH1-deficient cells, we propose inhibition of template switching is sensitizing
248 FBH1-deficient cells to HU. Template switching restarts stalled replication forks, bypasses DNA
249 lesions and fills ssDNA gaps during S phase[21,32,59]. One possibility is that the anti-recombinase
250 activity of FBH1 disassembles RAD51 presynaptic filaments to inhibit template switching. In *S.*
251 *pombe*, Fbh1 plays a similar role inhibiting HR at stalled replication forks[30,31,60,61]. Indeed,
252 upregulation of RAD51 and template switching can lead to resistance to chemotherapeutics[62–65].

253 Alternatively, FBH1-deficient cells may depend on UBC13-mediated template switching in
254 response to replication stress. Previous studies have shown that PRIMPOL-mediated DNA
255 synthesis is upregulated in cells lacking fork regression mediated by HLTF, RAD51 and
256 SMARCAL1[19–21]. Excessive PRIMPOL activity promotes resistance to replication stress in a
257 BRCA1-deficient background[66]. The resulting ssDNA gaps left by PRIMPOL can be filled by
258 template switching during S phase[21]. FBH1 promotes fork regression in an HLTF-independent
259 pathway[8,12]. Therefore, it is possible FBH1 KO cells are reliant on template switching to fill
260 ssDNA gaps that arise due to PRIMPOL-dependent synthesis due to the defect in fork
261 regression. Future work is warranted to distinguish between these models.
262 Hemizygous and homozygous loss of FBH1 was found in up to 63% of cell lines derived
263 from melanoma. FBH1 protects melanocytes from UV-mediated transformation and FBH1-
264 deficient melanoma cell lines are resistant to replication stress induced by HU[38]. Our results here
265 suggest UBC13-dependent template switching may be a potential target to sensitize FBH1-
266 deficient tumors to replication stress. Future studies will determine if template switching is
267 driving UV resistance and malignant transformation of melanocytes.
268
269 **Limitations of Study**
270 Finally, there are limitations to the current study. First, we were unable to directly test the
271 role of the anti-recombinase activity of FBH1 in promoting resistance to HU. Mutations in FBH1
272 that disrupt the anti-recombinase activity of FBH1 disrupt other functions. The helicase activity
273 of FBH1 is required for both the anti-recombinase activity of FBH1 and to promote fork
274 regression[8,39,41]. Ubiquitination of RAD51 to prevent re-associated of DNA after removal by
275 FBH1 requires the FBOX; however, FBH1 is also ubiquitinated to negatively regulate anti-

276 recombinase activity[40,42]. Second, inhibition of RAD51 and UBC13 is inhibiting other pathways
277 besides template switching. These limitations highlight the need for generation of a separation-
278 of-function mutant that disrupts only the anti-recombinase activity of FBH1.
279

280 **ACKNOWLEDGEMENTS**

281 We would like to thank Garrett Buzzard and Michael Sehorn for purification of GST-tagged
282 FBH1-N250 and FBH1 polyclonal antibodies. We thank Michael Sehorn for feedback on a draft
283 of the manuscript. This work is funded in part by the American Cancer Society Research Scholar
284 Grant RSG-21-175-01-DMC (https://doi.org/10.53354/pc.gr.152677) to J.M.M and NIGMS
285 (R35 GM142512-01) to J.M.M.
286

287 **AUTHOR CONTRIBUTIONS**

288 ALH, AB, and JMM designed the project. ALH, AB, and TJM conducted the experiments and
289 analyzed data. JMM supervised the project. The manuscript was written by ALH, AB, and JMM.
290

291 **RESOURCE AVAILABILITY**

292

293 *Lead Contact*

294 Further information and requests for resources and reagents should be directed to and will be
295 fulfilled by the lead contact, Jennifer Mason, PhD (jmason4@clemson.edu).
296

297 *Materials availability*

298 Cell lines generated in this study can be made available by contacting the lead contact and
299 completing a Materials Transfer Agreement.
300
301 *Data and code availability*
302 This paper does not provide any original code or algorithms. All data will be available from the
303 lead contact upon request.
304
305 **MATERIAL AND METHODS**
306 **Experimental Model and Subject Details**
307 U2OS cell lines were cultured in Dulbecco's Modified Eagle's Medium (DMEM) supplemented
308 with 10% FBS. RPE-1 cells were cultured in DMEM/F-12 media supplemented with 10% FBS.
309 All cells were cultured at 37ºC with 5% CO_2. The U2OS FBH1-KO cell line was generated using
310 CRISPR-Cas9 technology.
311
312 **RNA Interference**
313 Cells (1.0-1.5X10^5) were plated in 6-well plates. After 24 hours, cells were transfected with
314 siRNAs using Lipofectamine RNAiMax (Invitrogen) following the manufacturer's instructions.
315 The siFBH1 final concentration was 75 nM[13]. The siUBC13 siRNA final concentration was 50
316 nM[21]. The All-Star negative control siRNA (Qiagen) was used as a control. Cells were replated
317 for assays 24 hours after the transfection.
318
319 **Drug Treatments**

320 B02 was and RI(dl)2 were resuspended in DMSO and stored at -20ºC. Hydroxyurea was
321 resuspended in UltraPure dH_2O and used immediately. Cells were treated either 24 hours
322 following plating or 48 hours following siRNA transfection. DMSO or indicated concentrations
323 of B02 and RI(dl)2 was added to the cells 30 minutes prior to the addition of hydroxyurea. Cells
324 were treated with 2 mM hydroxyurea for 24 hours with or without DMSO or indicated
325 concentrations of B02 and RI(dl)2.
326
327 **Generation of FBH1 polyclonal antibodies**
328 The N-terminal 250 amino acids of human FBH1 were cloned in to a pGEX6p-1 expression
329 vector using Gibson assembly. Primers used to amplify the FBH1 fragment were
330 FBH1_pGEX6_F (5' TTCTGTTCCAGGGGCCCCTGGGATCCagctacgaggtgacttcag) and
331 FBH1_N250_pGEX__R (5' GTCGACCCGGGAATTCCGGGGATCCtcaaagcccatagtatgagtcag).
332 GST-FBH1[1-250] in the pGEX6P-1 vector (Amersham/GE Healthcare/Cytiva) was introduced
333 into BL21:DE3 Rosetta cells (Novagen). The cells were grown at 37 °C to an OD_{600} of 0.8 and
334 induced with 0.4 mM IPTG for 16 h at 16 °C. All the steps of the purification were performed at
335 4 °C. A 10 g pellet of cells was suspended in 50 mL of cell breakage buffer (50 mM Tris-HCl,
336 pH 7.5, 10% sucrose, 2 mM EDTA, 250 mM KCl, 0.01% IgePal, 1 mM DTT, 1 mM
337 Phenylmethulsulfonyl fluoride, 0.5 mM benzamidine and 5 μg/mL each of aprotinin,
338 chymostatin, leupeptin, and pepstatin). The cells were sonicated and the crude lysate was
339 centrifuged at 100,000 x g for 90 min. The clarified lysate was incubated with 1 mL of
340 glutathione Sepharose (Cytiva) with constant agitation. The matrix was poured into a 1 cm
341 column and washed with 10 mLs Buffer A (50 mM Tris-HCl, pH8.0, 10% glycerol, 1 mM
342 EDTA, 1 mM DTT, and 0.01% IgePal) containing 1 M KCl and then 5 mL of Buffer A

343 containing 300 mM KCl. The bound GST-FBH1[1-250] was eluted with 6 mL of 10 mM
344 glutathione in Buffer A containing 300 mM KCl. The fractions containing GST-FBH1[1-250]
345 were pooled and concentrated in an Amicon Ultra microconcentrator to 500 µL and subjected to
346 size exclusion chromatography on a 40 mL Sephacryl S200 column in Buffer A containing 300
347 mM KCl. The fractions containing GST-FBH1[1-250] were pooled and concentrated as before
348 to 8 mg/mL, and stored in small aliquots at -80 °C. ~1 mg of GST-FBH1[1-250] was used to
349 generate antibodies from Pacific Immunology. Purified GST-FBH1[1-250] was coupled to
350 CNBr activated Sepharose per the manufacturer's instructions. Serum was applied to a 1 mL of
351 the matrix in a 1 cm column. The matrix was washed with 10 mL PBS (10 mM Na_2HPO_4, pH
352 7.4, 2.7 mM KCl, 137 mM NaCl, 0.05 % TWEEN) followed by elution with 166 mM MES pH
353 6.0 containing 100 mM diethylamine. The fractions that contained the antibodies were pooled
354 and dialyzed against PBS. The dialyzed antibodies were concentrated in a Amicon Ultra
355 microconcentrator, supplemented with 0.01% sodium azide and stored in small aliquots at 4 °C.
356

357 **Immunoblotting**

358 Cells were lysed by resuspending pellets in 100 µL 1:1 2xSDS:1xPBS per $1x10^6$ cells and boiled
359 for 5 minutes. Denatured proteins were run on an SDS-PAGE gel and transferred to PVDF
360 membrane. Membranes were probed with primary antibodies (diluted in 5% milk in 1xTBST) for
361 1 hour at room temperature to overnight at 4ºC. The membrane washed three times with 1xTBST
362 and probed with HRP-conjugated secondary antibodies (WesternSure, Licor) for one hour at
363 room temperature. Membrane was washed three times with 1xTBST, incubated with 1:1 ECL
364 reagents for 5 minutes at room temperature, and imaged using a Licor C-Digit scanner. The
365 primary antibodies used were FBH1 (1:500), Alpha-tubulin (Novus Biologicals, NB100-

366 690,1:1000), UBC13 (Santa Cruz, Sc376470, 1:1000), and Vinculin (Cell Signaling
367 Technologies,13901S 1:1000).
368
369 **Immunofluorescence**
370 Cells ($5.0x10^4$) plated on glass coverslips in 12-well plates one day prior to drug treatment.
371 Following the drug treatment, cells were washed with PBS and incubated in HEPES/TritonX-
372 100 Buffer (20 mM HEPES, ph7.4, 0.5% Triton-X 100, 50mM NaCl, 3 mM MgCl2, 300 mM
373 sucrose in water) for 10 minutes at room temperature. Cells were fixed with 3%
374 paraformaldehyde, 3.4% sucrose in 1xPBS for 10 minutes at room temperature. Cells were
375 washed twice with 1xPBS. For PCNA staining, cells were treated with ice cold 100% Methanol
376 for 10 minutes followed by two additional PBS washes. Cells were incubated with 1% BSA in
377 1xPBS for 20 minutes at room temperature. Cells were incubated with the primary antibodies
378 (diluted in 1% BSA) for 1 hour at room temperature or overnight at 4ºC and were washed three
379 times with 1xPBS. Coverslips were incubated with the secondary antibodies (diluted in 1% BSA)
380 for 1 hour at room temperature away from light and were washed 3 times with 1xPBS. Once dry,
381 coverslips were mounted with Vectashield + DAPI and sealed with nail polish. Images acquired
382 on Zeiss Axio M2 upright fluorescence microscope and data quantified using ImageJ software.
383 The primary antibodies used were Mouse anti-RPA32/RPA2 [9H8] (Abcam Ab2175, 1:1000),
384 Rabbit phospho-RPA32 (Ser33) polyclonal (Bethyl Laboratories, A300-246A-T,1:1000), Rabbit
385 phospho-RPA32 (Ser4, Ser8) polyclonal (Bethyl Laboratories, A300-245A-M, 1:1000), Rabbit
386 anti-PCNA (Abcam, Ab18197, 1:1000), and Mouse anti-gamma H2AX (phospho S139) [9F3]
387 (Abcam, Ab26350, 1:1000).
388

389 **TUNEL Assay**

390 TUNEL assay performed using Click-iT Plus TUNEL assay kit (Invitrogen) following
391 manufacturer's protocol. All incubations longer than 5 minutes were performed in a humidity
392 chamber. Cells were lysed and fixed as described above. Coverslips were incubated with TdT
393 Reaction Buffer for 10 minutes at 37ºC. Excess buffer was removed, and the TdT reaction
394 mixture (TdT Reaction Buffer, EdUTP, and TdT Enzyme) was added to each coverslip.
395 Coverslips were incubated for 60 minutes at 37ºC. Coverslips were rinsed once with dH_2O,
396 followed by a 5-minute wash with 3% BSA, 0.1% Triton X-100 in 1xPBS for 5 minutes at room
397 temperature. Coverslips are rinsed with 1xPBS and incubated with Click-iT PLUS TUNEL
398 Reaction cocktail (Click-iT supermix, 10x Click-iT Additive) for 30 minutes at 37ºC. Coverslips
399 washed with 3% BSA in 1xPBS for 5 minutes, followed by a rinse with 1xPBS. Slides were next
400 stained for PCNA as the cell cycle indicator using protocol described previously.

401

402 **Survival Assay**

403 Cells were plated in 96-well black, clear bottom plates (Corning) 24 hours post-transfection.
404 100-1000 cells plated per well in triplicate. 48 hours post-transfection cells were treated with 0-4
405 mM HU for 24 hours. Following treatment, cells were washed twice with 1xPBS and allowed to
406 recover in fresh media for 4-5 days. 20 µL of CellTiter-Blue reagent was added to each well
407 containing cells plus 3 no-cell control wells and incubated at 37ºC for 2 hours. The reaction was
408 stopped by adding 50 µL of 3% SDS to each well. On a Synergy H1 plate reader, plates were
409 shaken for 10 seconds, and endpoint fluorescence read at 570/600. Fluorescence data used to
410 quantify survival of each sample.

411

412 **Quantification and Statistical Analysis**

413 All microscopy images were scored using ImageJ software. Statistical analysis was performed
414 using Prism software, and the tests performed are indicated in figure legends. All experiments
415 consist of three independent experiments.

REFERENCES

1. Zeman, M.K., and Cimprich, K.A. (2014). Causes and consequences of replication stress. Nat Cell Biol *16*, 2–9. 10.1038/ncb2897.

2. Muñoz, S., and Méndez, J. (2017). DNA replication stress: from molecular mechanisms to human disease. Chromosoma *126*, 1–15. 10.1007/s00412-016-0573-x.

3. Fitzgerald, D.M., Hastings, P.J., and Rosenberg, S.M. (2017). Stress-Induced Mutagenesis: Implications in Cancer and Drug Resistance. Annu. Rev. Cancer Biol. *1*, 119–140. 10.1146/annurev-cancerbio-050216-121919.

4. Fujiwara, Y., and Tatsumi, M. (1976). Replicative bypass repair of ultraviolet damage to DNA of mammalian cells: Caffeine sensitive and caffeine resistant mechanisms. Mutation Research/Fundamental and Molecular Mechanisms of Mutagenesis *37*, 91–109. 10.1016/0027-5107(76)90058-0.

5. Zellweger, R., Dalcher, D., Mutreja, K., Berti, M., Schmid, J.A., Herrador, R., Vindigni, A., and Lopes, M. (2015). Rad51-mediated replication fork reversal is a global response to genotoxic treatments in human cells. Journal of Cell Biology *208*, 563–579. 10.1083/jcb.201406099.

6. Weston, R., Peeters, H., and Ahel, D. (2012). ZRANB3 is a structure-specific ATP-dependent endonuclease involved in replication stress response. Genes Dev. *26*, 1558–1572. 10.1101/gad.193516.112.

7. Kile, A.C., Chavez, D.A., Bacal, J., Eldirany, S., Korzhnev, D.M., Bezsonova, I., Eichman, B.F., and Cimprich, K.A. (2015). HLTF's Ancient HIRAN Domain Binds 3′ DNA Ends to Drive Replication Fork Reversal. Molecular Cell *58*, 1090–1100. 10.1016/j.molcel.2015.05.013.

8. Fugger, K., Mistrik, M., Neelsen, K.J., Yao, Q., Zellweger, R., Kousholt, A.N., Haahr, P., Chu, W.K., Bartek, J., Lopes, M., et al. (2015). FBH1 Catalyzes Regression of Stalled Replication Forks. Cell Reports *10*, 1749–1757. 10.1016/j.celrep.2015.02.028.

9. Vujanovic, M., Krietsch, J., Raso, M.C., Terraneo, N., Zellweger, R., Schmid, J.A., Taglialatela, A., Huang, J.-W., Holland, C.L., Zwicky, K., et al. (2017). Replication Fork Slowing and Reversal upon DNA Damage Require PCNA Polyubiquitination and ZRANB3 DNA Translocase Activity. Molecular Cell *67*, 882-890.e5. 10.1016/j.molcel.2017.08.010.

10. Bai, G., Kermi, C., Stoy, H., Schiltz, C.J., Bacal, J., Zaino, A.M., Hadden, M.K., Eichman, B.F., Lopes, M., and Cimprich, K.A. (2020). HLTF Promotes Fork Reversal, Limiting Replication Stress Resistance and Preventing Multiple Mechanisms of Unrestrained DNA Synthesis. Molecular Cell *78*, 1237-1251.e7. 10.1016/j.molcel.2020.04.031.

11. Kolinjivadi, A.M., Sannino, V., De Antoni, A., Zadorozhny, K., Kilkenny, M., Técher, H., Baldi, G., Shen, R., Ciccia, A., Pellegrini, L., et al. (2017). Smarcal1-Mediated Fork

Reversal Triggers Mre11-Dependent Degradation of Nascent DNA in the Absence of Brca2 and Stable Rad51 Nucleofilaments. Molecular Cell *67*, 867-881.e7. 10.1016/j.molcel.2017.07.001.

12. Liu, W., Krishnamoorthy, A., Zhao, R., and Cortez, D. (2020). Two replication fork remodeling pathways generate nuclease substrates for distinct fork protection factors. Sci. Adv. *6*, eabc3598. 10.1126/sciadv.abc3598.

13. Mason, J.M., Chan, Y.-L., Weichselbaum, R.W., and Bishop, D.K. (2019). Non-enzymatic roles of human RAD51 at stalled replication forks. Nat Commun *10*, 4410. 10.1038/s41467-019-12297-0.

14. Hashimoto, Y., Ray Chaudhuri, A., Lopes, M., and Costanzo, V. (2010). Rad51 protects nascent DNA from Mre11-dependent degradation and promotes continuous DNA synthesis. Nat Struct Mol Biol *17*, 1305–1311. 10.1038/nsmb.1927.

15. Schlacher, K., Christ, N., Siaud, N., Egashira, A., Wu, H., and Jasin, M. (2011). Double-Strand Break Repair-Independent Role for BRCA2 in Blocking Stalled Replication Fork Degradation by MRE11. Cell *145*, 529–542. 10.1016/j.cell.2011.03.041.

16. Zhang, S., Zhou, T., Wang, Z., Yi, F., Li, C., Guo, W., Xu, H., Cui, H., Dong, X., Liu, J., et al. (2021). Post-Translational Modifications of PCNA in Control of DNA Synthesis and DNA Damage Tolerance-the Implications in Carcinogenesis. Int. J. Biol. Sci. *17*, 4047–4059. 10.7150/ijbs.64628.

17. Bianchi, J., Rudd, S.G., Jozwiakowski, S.K., Bailey, L.J., Soura, V., Taylor, E., Stevanovic, I., Green, A.J., Stracker, T.H., Lindsay, H.D., et al. (2013). PrimPol Bypasses UV Photoproducts during Eukaryotic Chromosomal DNA Replication. Molecular Cell *52*, 566–573. 10.1016/j.molcel.2013.10.035.

18. Piberger, A.L., Bowry, A., Kelly, R.D.W., Walker, A.K., González-Acosta, D., Bailey, L.J., Doherty, A.J., Méndez, J., Morris, J.R., Bryant, H.E., et al. (2020). PrimPol-dependent single-stranded gap formation mediates homologous recombination at bulky DNA adducts. Nat Commun *11*, 5863. 10.1038/s41467-020-19570-7.

19. Quinet, A., Tirman, S., Jackson, J., Šviković, S., Lemaçon, D., Carvajal-Maldonado, D., González-Acosta, D., Vessoni, A.T., Cybulla, E., Wood, M., et al. (2020). PRIMPOL-Mediated Adaptive Response Suppresses Replication Fork Reversal in BRCA-Deficient Cells. Molecular Cell *77*, 461-474.e9. 10.1016/j.molcel.2019.10.008.

20. Vallerga, M.B., Mansilla, S.F., Federico, M.B., Bertolin, A.P., and Gottifredi, V. (2015). Rad51 recombinase prevents Mre11 nuclease-dependent degradation and excessive PrimPol-mediated elongation of nascent DNA after UV irradiation. Proc. Natl. Acad. Sci. U.S.A. *112*. 10.1073/pnas.1508543112.

21. Tirman, S., Quinet, A., Wood, M., Meroni, A., Cybulla, E., Jackson, J., Pegoraro, S., Simoneau, A., Zou, L., and Vindigni, A. (2021). Temporally distinct post-replicative repair

mechanisms fill PRIMPOL-dependent ssDNA gaps in human cells. Molecular Cell *81*, 4026-4040.e8. 10.1016/j.molcel.2021.09.013.

22. Branzei, D., and Foiani, M. (2007). Template Switching: From Replication Fork Repair to Genome Rearrangements. Cell *131*, 1228–1230. 10.1016/j.cell.2007.12.007.

23. Motegi, A., Liaw, H.-J., Lee, K.-Y., Roest, H.P., Maas, A., Wu, X., Moinova, H., Markowitz, S.D., Ding, H., Hoeijmakers, J.H.J., et al. (2008). Polyubiquitination of proliferating cell nuclear antigen by HLTF and SHPRH prevents genomic instability from stalled replication forks. Proc. Natl. Acad. Sci. U.S.A. *105*, 12411–12416. 10.1073/pnas.0805685105.

24. Hofmann, R.M., and Pickart, C.M. (1999). Noncanonical MMS2-Encoded Ubiquitin-Conjugating Enzyme Functions in Assembly of Novel Polyubiquitin Chains for DNA Repair. Cell *96*, 645–653. 10.1016/S0092-8674(00)80575-9.

25. Ulrich, H.D. (2000). Two RING finger proteins mediate cooperation between ubiquitin-conjugating enzymes in DNA repair. The EMBO Journal *19*, 3388–3397. 10.1093/emboj/19.13.3388.

26. Broomfield, S., Chow, B.L., and Xiao, W. (1998). *MMS2* , encoding a ubiquitin-conjugating-enzyme-like protein, is a member of the yeast error-free postreplication repair pathway. Proc. Natl. Acad. Sci. U.S.A. *95*, 5678–5683. 10.1073/pnas.95.10.5678.

27. Papouli, E., Chen, S., Davies, A.A., Huttner, D., Krejci, L., Sung, P., and Ulrich, H.D. (2005). Crosstalk between SUMO and Ubiquitin on PCNA Is Mediated by Recruitment of the Helicase Srs2p. Molecular Cell *19*, 123–133. 10.1016/j.molcel.2005.06.001.

28. Krejci, L., Van Komen, S., Li, Y., Villemain, J., Reddy, M.S., Klein, H., Ellenberger, T., and Sung, P. (2003). DNA helicase Srs2 disrupts the Rad51 presynaptic filament. Nature *423*, 305–309. 10.1038/nature01577.

29. Pfander, B., Moldovan, G.-L., Sacher, M., Hoege, C., and Jentsch, S. (2005). SUMO-modified PCNA recruits Srs2 to prevent recombination during S phase. Nature *436*, 428–433. 10.1038/nature03665.

30. Veaute, X., Jeusset, J., Soustelle, C., Kowalczykowski, S.C., Le Cam, E., and Fabre, F. (2003). The Srs2 helicase prevents recombination by disrupting Rad51 nucleoprotein filaments. Nature *423*, 309–312. 10.1038/nature01585.

31. Lorenz, A., Osman, F., Folkyte, V., Sofueva, S., and Whitby, M.C. (2009). Fbh1 Limits Rad51-Dependent Recombination at Blocked Replication Forks. Mol Cell Biol *29*, 4742–4756. 10.1128/MCB.00471-09.

32. Jalan, M., Oehler, J., Morrow, C.A., Osman, F., and Whitby, M.C. (2019). Factors affecting template switch recombination associated with restarted DNA replication. eLife *8*, e41697. 10.7554/eLife.41697.

33. Tsutsui, Y., Kurokawa, Y., Ito, K., Siddique, Md.S.P., Kawano, Y., Yamao, F., and Iwasaki, H. (2014). Multiple Regulation of Rad51-Mediated Homologous Recombination by Fission Yeast Fbh1. PLoS Genet *10*, e1004542. 10.1371/journal.pgen.1004542.

34. Kim, J.-H. (2004). SCFhFBH1 can act as helicase and E3 ubiquitin ligase. Nucleic Acids Research *32*, 2287–2297. 10.1093/nar/gkh534.

35. Kim, J., Kim, J.-H., Lee, S.-H., Kim, D.-H., Kang, H.-Y., Bae, S.-H., Pan, Z.-Q., and Seo, Y.-S. (2002). The Novel Human DNA Helicase hFBH1 Is an F-box Protein. Journal of Biological Chemistry *277*, 24530–24537. 10.1074/jbc.M201612200.

36. Fugger, K., Kit Chu, W., Haahr, P., Nedergaard Kousholt, A., Beck, H., Payne, M.J., Hanada, K., Hickson, I.D., and Storgaard Sørensen, C. (2013). FBH1 co-operates with MUS81 in inducing DNA double-strand breaks and cell death following replication stress. Nat Commun *4*, 1423. 10.1038/ncomms2395.

37. Jeong, Y.-T., Rossi, M., Cermak, L., Saraf, A., Florens, L., Washburn, M.P., Sung, P., Schildkraut, C.L., and Pagano, M. (2013). FBH1 promotes DNA double-strand breakage and apoptosis in response to DNA replication stress. Journal of Cell Biology *200*, 141–149. 10.1083/jcb.201209002.

38. Jeong, Y.-T., Cermak, L., Guijarro, M., Hernando, E., and Pagano, M. (2013). FBH1 protects melanocytes from transformation and is deregulated in melanomas. Cell Cycle *12*, 1128–1132. 10.4161/cc.24165.

39. Simandlova, J., Zagelbaum, J., Payne, M.J., Chu, W.K., Shevelev, I., Hanada, K., Chatterjee, S., Reid, D.A., Liu, Y., Janscak, P., et al. (2013). FBH1 Helicase Disrupts RAD51 Filaments in Vitro and Modulates Homologous Recombination in Mammalian Cells. Journal of Biological Chemistry *288*, 34168–34180. 10.1074/jbc.M113.484493.

40. Masuda-Ozawa, T., Hoang, T., Seo, Y.-S., Chen, L.-F., and Spies, M. (2013). Single-molecule sorting reveals how ubiquitylation affects substrate recognition and activities of FBH1 helicase. Nucleic Acids Research *41*, 3576–3587. 10.1093/nar/gkt056.

41. Fugger, K., Mistrik, M., Danielsen, J.R., Dinant, C., Falck, J., Bartek, J., Lukas, J., and Mailand, N. (2009). Human Fbh1 helicase contributes to genome maintenance via pro- and anti-recombinase activities. Journal of Cell Biology *186*, 655–663. 10.1083/jcb.200812138.

42. Chu, W.K., Payne, M.J., Beli, P., Hanada, K., Choudhary, C., and Hickson, I.D. (2015). FBH1 influences DNA replication fork stability and homologous recombination through ubiquitylation of RAD51. Nat Commun *6*, 5931. 10.1038/ncomms6931.

43. Huang, F., Motlekar, N.A., Burgwin, C.M., Napper, A.D., Diamond, S.L., and Mazin, A.V. (2011). Identification of Specific Inhibitors of Human RAD51 Recombinase Using High-Throughput Screening. ACS Chem. Biol. *6*, 628–635. 10.1021/cb100428c.

44. Vassin, V.M., Anantha, R.W., Sokolova, E., Kanner, S., and Borowiec, J.A. (2009). Human RPA phosphorylation by ATR stimulates DNA synthesis and prevents ssDNA accumulation during DNA-replication stress. Journal of Cell Science *122*, 4070–4080. 10.1242/jcs.053702.

45. Toledo, L.I., Altmeyer, M., Rask, M.-B., Lukas, C., Larsen, D.H., Povlsen, L.K., Bekker-Jensen, S., Mailand, N., Bartek, J., and Lukas, J. (2013). ATR Prohibits Replication Catastrophe by Preventing Global Exhaustion of RPA. Cell *155*, 1088–1103. 10.1016/j.cell.2013.10.043.

46. Regairaz, M., Zhang, Y.-W., Fu, H., Agama, K.K., Tata, N., Agrawal, S., Aladjem, M.I., and Pommier, Y. (2011). Mus81-mediated DNA cleavage resolves replication forks stalled by topoisomerase I–DNA complexes. Journal of Cell Biology *195*, 739–749. 10.1083/jcb.201104003.

47. Ashley, A.K., Shrivastav, M., Nie, J., Amerin, C., Troksa, K., Glanzer, J.G., Liu, S., Opiyo, S.O., Dimitrova, D.D., Le, P., et al. (2014). DNA-PK phosphorylation of RPA32 Ser4/Ser8 regulates replication stress checkpoint activation, fork restart, homologous recombination and mitotic catastrophe. DNA Repair *21*, 131–139. 10.1016/j.dnarep.2014.04.008.

48. Rogakou, E.P., Pilch, D.R., Orr, A.H., Ivanova, V.S., and Bonner, W.M. (1998). DNA Double-stranded Breaks Induce Histone H2AX Phosphorylation on Serine 139. Journal of Biological Chemistry *273*, 5858–5868. 10.1074/jbc.273.10.5858.

49. Di Marco, S., Hasanova, Z., Kanagaraj, R., Chappidi, N., Altmannova, V., Menon, S., Sedlackova, H., Langhoff, J., Surendranath, K., Hühn, D., et al. (2017). RECQ5 Helicase Cooperates with MUS81 Endonuclease in Processing Stalled Replication Forks at Common Fragile Sites during Mitosis. Molecular Cell *66*, 658-671.e8. 10.1016/j.molcel.2017.05.006.

50. Chavdarova, M., Marini, V., Sisakova, A., Sedlackova, H., Vigasova, D., Brill, S.J., Lisby, M., and Krejci, L. (2015). Srs2 promotes Mus81–Mms4-mediated resolution of recombination intermediates. Nucleic Acids Research *43*, 3626–3642. 10.1093/nar/gkv198.

51. Cloud, V., Chan, Y.-L., Grubb, J., Budke, B., and Bishop, D.K. (2012). Rad51 Is an Accessory Factor for Dmc1-Mediated Joint Molecule Formation During Meiosis. Science *337*, 1222–1225. 10.1126/science.1219379.

52. Lv, W., Budke, B., Pawlowski, M., Connell, P.P., and Kozikowski, A.P. (2016). Development of Small Molecules that Specifically Inhibit the D-loop Activity of RAD51. J. Med. Chem. *59*, 4511–4525. 10.1021/acs.jmedchem.5b01762.

53. Branzei, D., and Szakal, B. (2016). DNA damage tolerance by recombination: Molecular pathways and DNA structures. DNA Repair *44*, 68–75. 10.1016/j.dnarep.2016.05.008.

54. Nayak, S., Calvo, J.A., Cong, K., Peng, M., Berthiaume, E., Jackson, J., Zaino, A.M., Vindigni, A., Hadden, M.K., and Cantor, S.B. (2020). Inhibition of the translesion synthesis polymerase REV1 exploits replication gaps as a cancer vulnerability. Sci. Adv. *6*, eaaz7808. 10.1126/sciadv.aaz7808.

55. Hodge, C.D., Spyracopoulos, L., and Glover, J.N.M. (2016). Ubc13: the Lys63 ubiquitin chain building machine. Oncotarget *7*, 64471–64504. 10.18632/oncotarget.10948.

56. Branzei, D. (2011). Ubiquitin family modifications and template switching. FEBS Letters *585*, 2810–2817. 10.1016/j.febslet.2011.04.053.

57. Fukushima, T., Matsuzawa, S., Kress, C.L., Bruey, J.M., Krajewska, M., Lefebvre, S., Zapata, J.M., Ronai, Z., and Reed, J.C. (2007). Ubiquitin-conjugating enzyme Ubc13 is a critical component of TNF receptor-associated factor (TRAF)-mediated inflammatory responses. Proc. Natl. Acad. Sci. U.S.A. *104*, 6371–6376. 10.1073/pnas.0700548104.

58. Ikura, T., Tashiro, S., Kakino, A., Shima, H., Jacob, N., Amunugama, R., Yoder, K., Izumi, S., Kuraoka, I., Tanaka, K., et al. (2007). DNA Damage-Dependent Acetylation and Ubiquitination of H2AX Enhances Chromatin Dynamics. Molecular and Cellular Biology *27*, 7028–7040. 10.1128/MCB.00579-07.

59. Vanoli, F., Fumasoni, M., Szakal, B., Maloisel, L., and Branzei, D. (2010). Replication and Recombination Factors Contributing to Recombination-Dependent Bypass of DNA Lesions by Template Switch. PLoS Genet *6*, e1001205. 10.1371/journal.pgen.1001205.

60. Osman, F., Dixon, J., Barr, A.R., and Whitby, M.C. (2005). The F-Box DNA Helicase Fbh1 Prevents Rhp51-Dependent Recombination without Mediator Proteins. Mol Cell Biol *25*, 8084–8096. 10.1128/MCB.25.18.8084-8096.2005.

61. Morishita, T., Furukawa, F., Sakaguchi, C., Toda, T., Carr, A.M., Iwasaki, H., and Shinagawa, H. (2005). Role of the *Schizosaccharomyces pombe* F-Box DNA Helicase in Processing Recombination Intermediates. Mol Cell Biol *25*, 8074–8083. 10.1128/MCB.25.18.8074-8083.2005.

62. Su, W.-P., Hsu, S.-H., Wu, C.-K., Chang, S.-B., Lin, Y.-J., Yang, W.-B., Hung, J.-J., Chiu, W.-T., Tzeng, S.-F., Tseng, Y.-L., et al. (2014). Chronic treatment with cisplatin induces replication-dependent sister chromatid recombination to confer cisplatin-resistant phenotype in nasopharyngeal carcinoma. Oncotarget *5*, 6323–6337. 10.18632/oncotarget.2210.

63. Hannay, J.A.F., Liu, J., Zhu, Q.-S., Bolshakov, S.V., Li, L., Pisters, P.W.T., Lazar, A.J.F., Yu, D., Pollock, R.E., and Lev, D. (2007). Rad51 overexpression contributes to chemoresistance in human soft tissue sarcoma cells: a role for p53/activator protein 2 transcriptional regulation. Molecular Cancer Therapeutics *6*, 1650–1660. 10.1158/1535-7163.MCT-06-0636.

64. Chen, G., Chen, J., Qiao, Y., Shi, Y., Liu, W., Zeng, Q., Xie, H., Shi, X., Sun, Y., Liu, X., et al. (2018). ZNF830 mediates cancer chemoresistance through promoting homologous-recombination repair. Nucleic Acids Research *46*, 1266–1279. 10.1093/nar/gkx1258.

65. Huang, W., Han, Z., Sun, Z., Feng, H., Zhao, L., Yuan, Q., Chen, C., Yu, S., Hu, Y., Yu, J., et al. (2022). PAK6 promotes homologous-recombination to enhance chemoresistance to oxaliplatin through ATR/CHK1 signaling in gastric cancer. Cell Death Dis *13*, 658. 10.1038/s41419-022-05118-8.

66. Mehta, K.P.M., Thada, V., Zhao, R., Krishnamoorthy, A., Leser, M., Lindsey Rose, K., and Cortez, D. (2022). CHK1 phosphorylates PRIMPOL to promote replication stress tolerance. Sci. Adv. *8*, eabm0314. 10.1126/sciadv.abm0314.

67. Jennings, L., Walters, H.A., and Mason, J.M. (2023). FBH1 deficiency sensitizes cells to WEE1 inhibition by promoting mitotic catastrophe (Cell Biology) 10.1101/2023.05.15.540841.

68. Schneider, C.A., Rasband, W.S., and Eliceiri, K.W. (2012). NIH Image to ImageJ: 25 years of image analysis. Nat Methods *9*, 671–675. 10.1038/nmeth.2089.

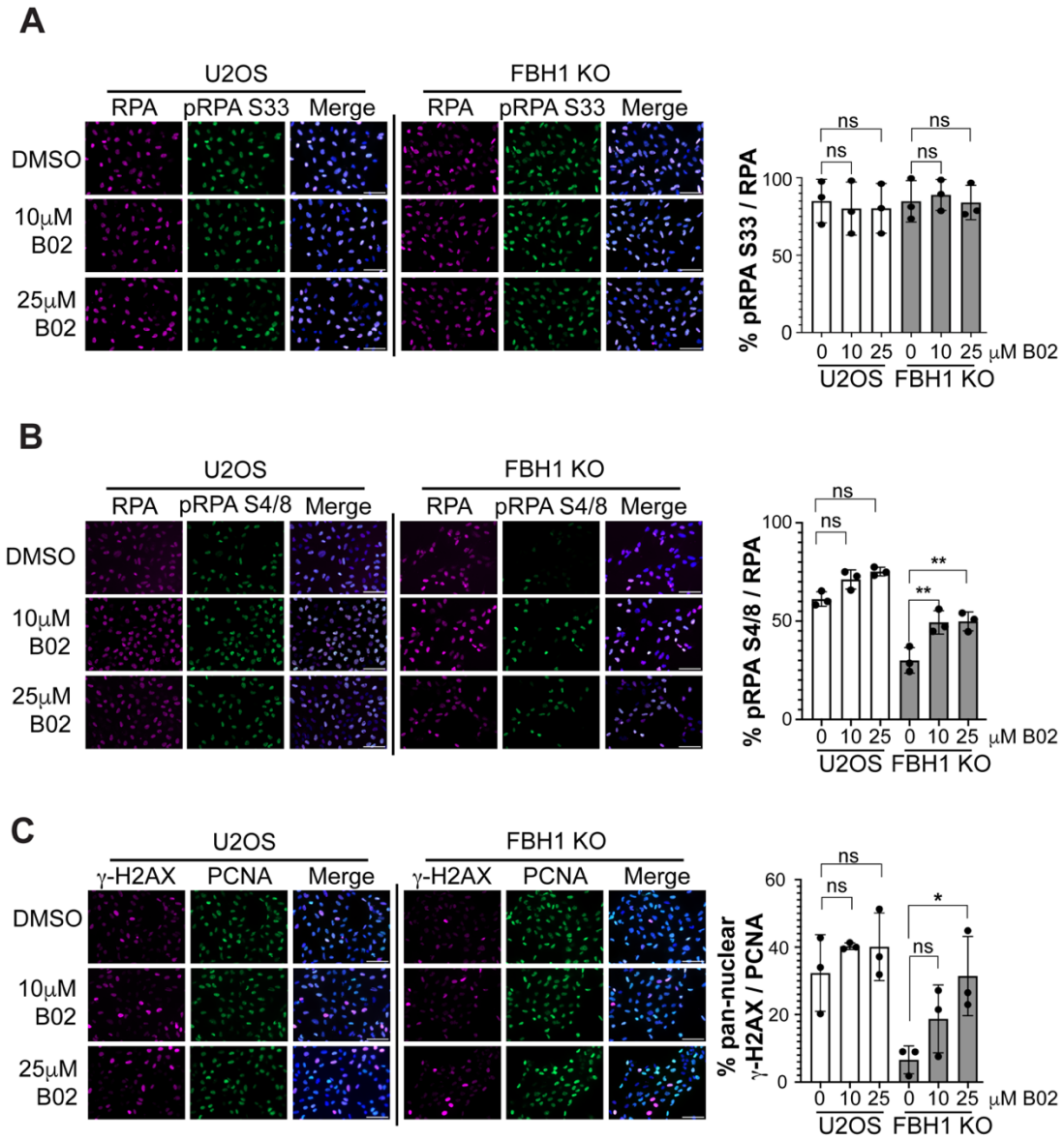

Figure 1. RAD51 DNA binding inhibition partially rescues DNA damage signaling in FBH1-KO cells. (A) Representative images of pRPA S33 (green) and RPA (magenta) in U2OS and FBH1 KO cells treated with 2mM HU +/- B02 for 24 hours. DNA is stained with DAPI (blue). Scale bar =100µm. Graph represents mean of three independent experiments. Error bars are standard deviation. Scale bar =100µm. **(B)** Representative images of pRPA S4/8 (green) and RPA (magenta) in U2OS and FBH1 KO cells treated with 2mM HU +/- B02 for 24 hours. DNA is stained with DAPI (blue). Scale bar =100µm. Graph represents mean of three independent experiments. Error bars are standard deviation. **(C)** Representative images of γ–H2AX (magenta) and PCNA (green) in U2OS and FBH1 KO cells treated with 2mM HU +/- B02 for 24 hours. DNA is stained with DAPI (blue) Scale bar =100µm. Graph represents mean of three independent experiments. Error bars are standard deviation. ns-not significant * $p<0.05$, ** $p<0.005$, Two-way ANOVA, Tukey.

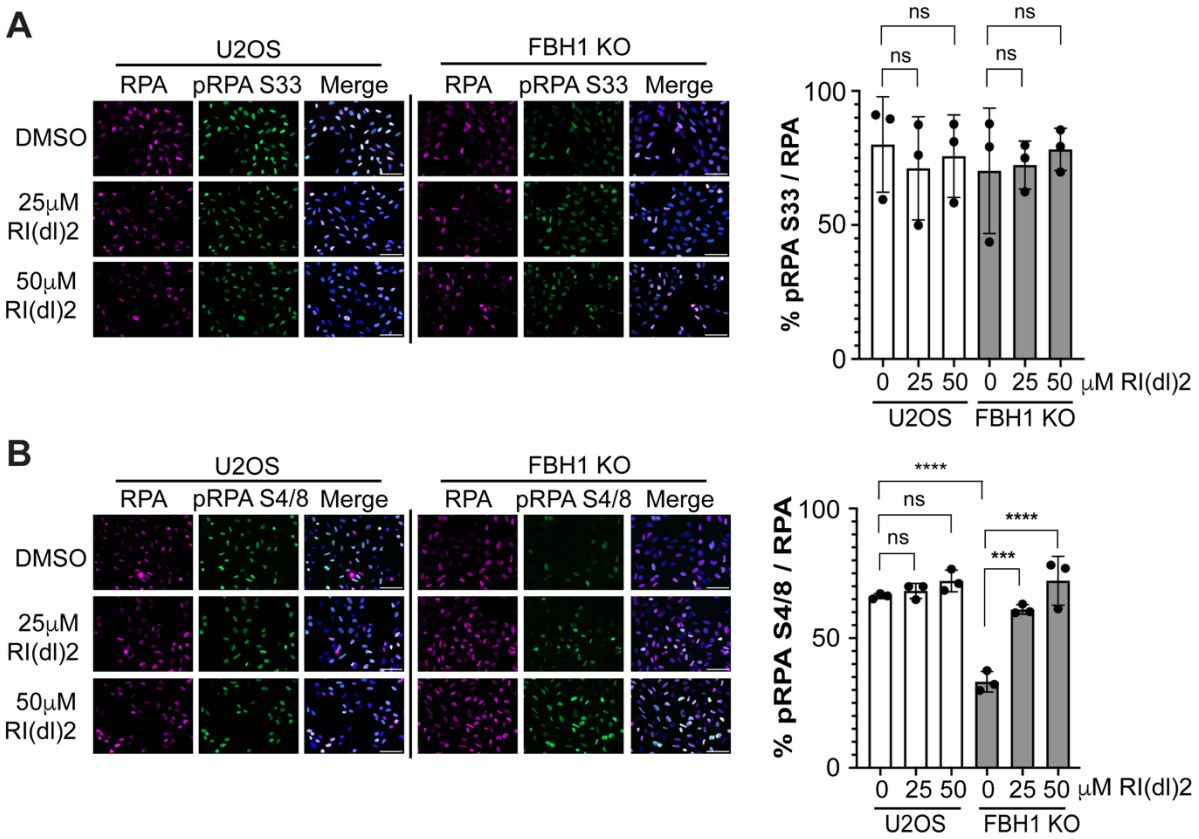

Figure 2. Inhibition of the strand exchange activity of RAD51 rescues DSB signaling in FBH1-KO cells. (A) Representative images of pRPA S33 (magenta) and RPA (green) in U2OS and FBH1 KO cells treated with 2mM HU +/- RI(dl)2 for 24 hours. DNA is stained with DAPI (blue). Scale bar =100µm. Graph represents mean of three independent experiments. Error bars are standard deviation. **(B)** Representative images of pRPA S4/8 (green) and RPA (magenta) in U2OS and FBH1 KO cells treated with 2mM HU +/- RI(dl)2 for 24 hours. DNA is stained with DAPI (blue). Scale bar =100µm. Graph represents mean of three independent experiments. Error bars are standard deviation. Error bars are standard deviation. ns – not significant. *** $p<0.0005$. **** $p<0.0001$. Two-way ANOVA, Tukey.

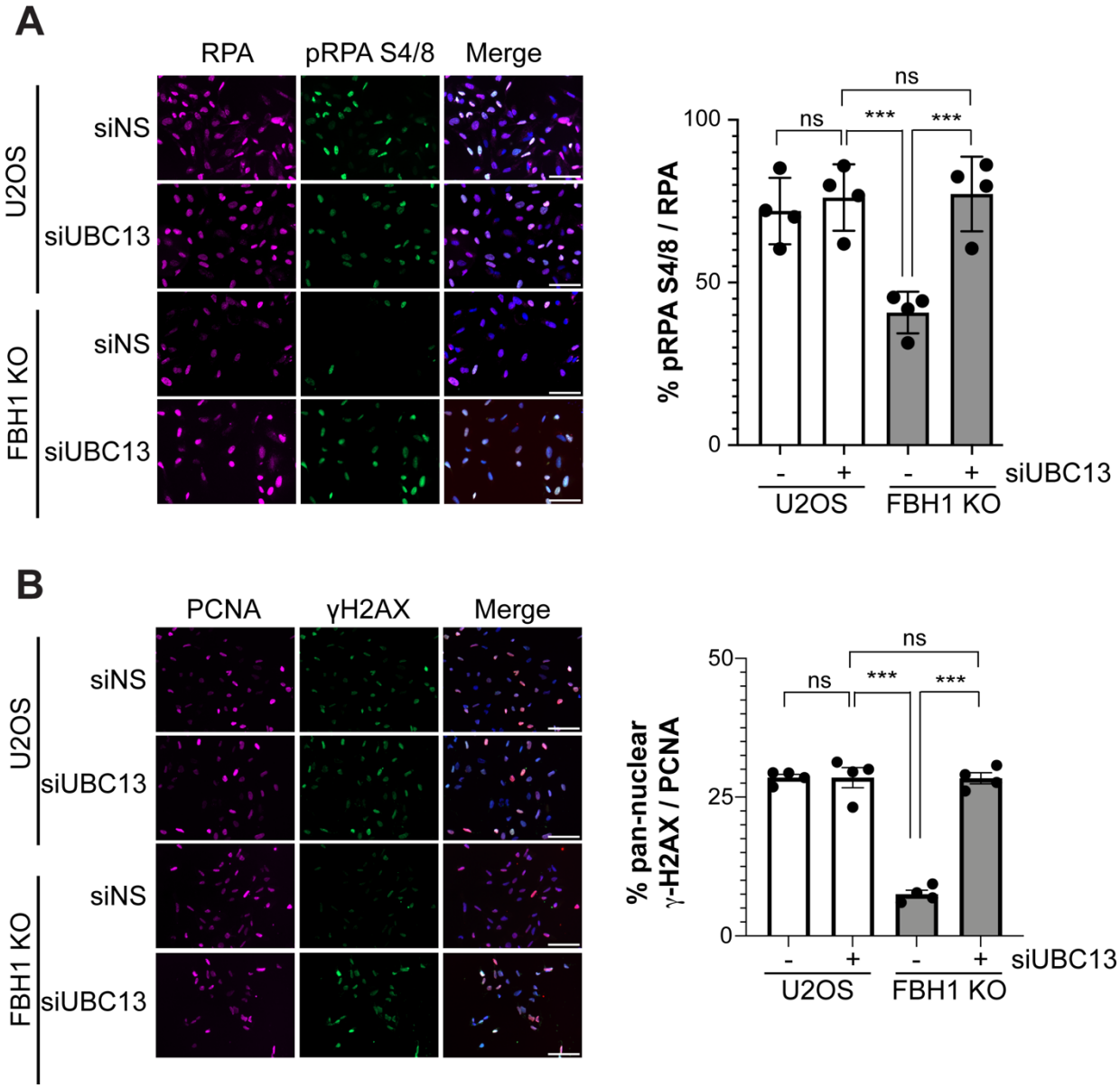

Figure 3. Depletion of UBC13 restores DSB signaling in FBH1-deficient cells. (A) Representative images of pRPA S4/8 (green) and RPA (magenta) in U2OS and FBH1 KO cells treated with 2mM HU for 24 hours. DNA is stained with DAPI (blue). Scale bar = 100µm. Graph represents mean of four independent experiments. Error bars are standard deviation. **(B)** Representative images of γ-H2AX (green) and PCNA (magenta) in U2OS and FBH1 KO cells treated with 2mM HU for 24 hours. DNA is stained with DAPI (blue). Scale bar =100µm. Graph represents mean of four independent experiments. Error bars are standard deviation. ns – not significant. ***p<0.0005, **** p<0.0001, Two-way ANOVA, Tukey.

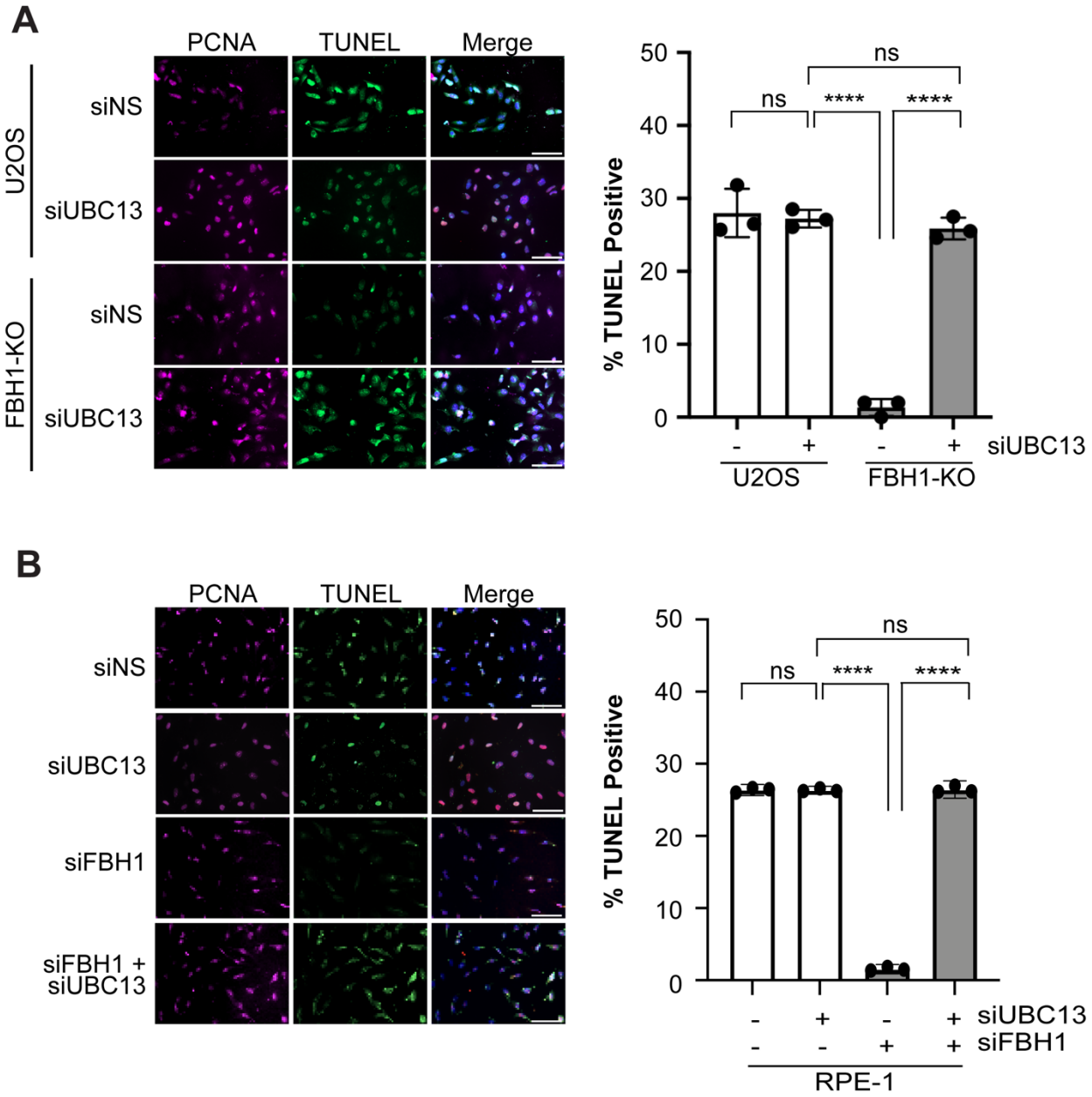

Figure 4: UBC13 depletion increases DSB formation in FBH1-deficient cells. (A) Representative images of TUNEL (green) and PCNA (magenta) in U2OS and FBH1 KO cells after treatment with 2 mM HU. DNA is stained with DAPI (blue). Graph represents mean of three independent experiments. Error bars are standard deviation. Scale bar =100 µm. **(B)** Representative images of TUNEL (Green) and PCNA (magenta) in RPE-1 cells transfected with the indicated siRNAs. DNA is stained with DAPI (blue). Scale bar =100 µm. Graph represents mean of three independent experiments. Error bars are standard deviation. Scale bar =100 µm. ns – not significant, **** - $p<0.0001$, Two-way ANOVA, Tukey.

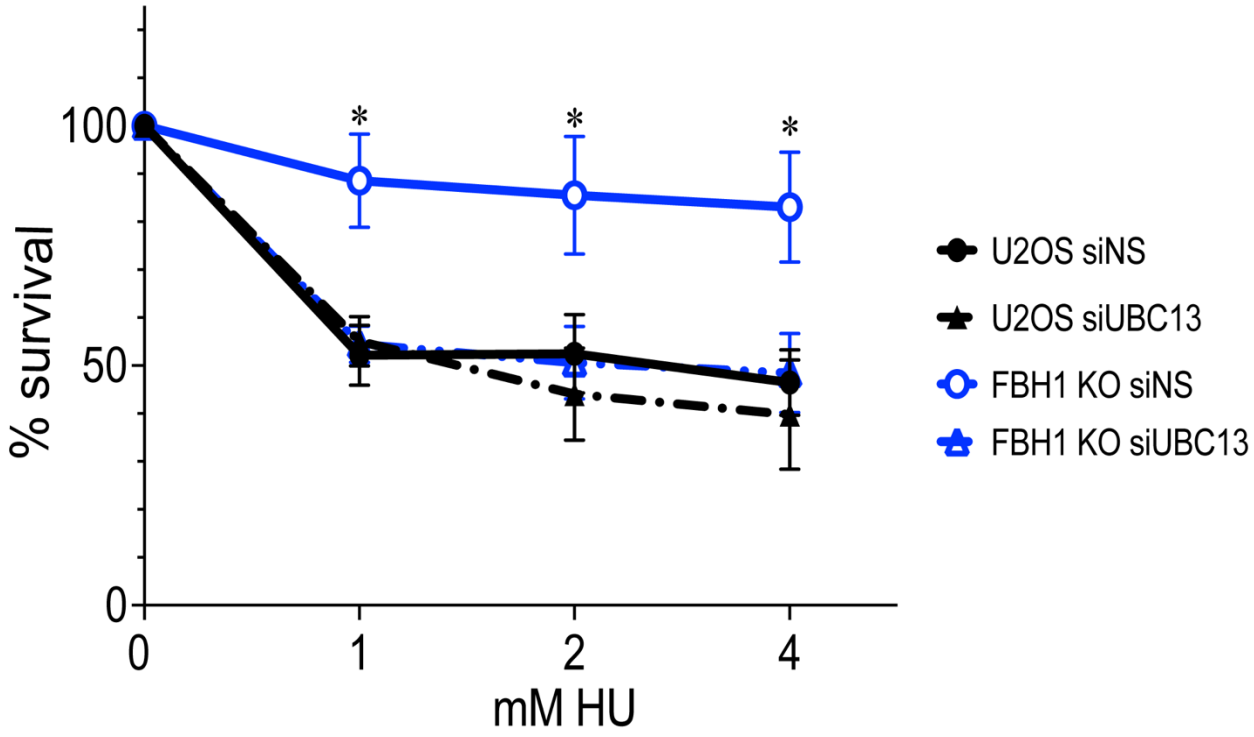

Figure 5. Depletion of UBC13 sensitizes FBH1-deficient cells to HU. Quantification of cellular survival in U2OS and FBH1 KO cells after treatment with indicated HU concentrations. Line represents average of three independent experiments. Error bars are standard error. *$p<0.05$, ANOVA, t-test.

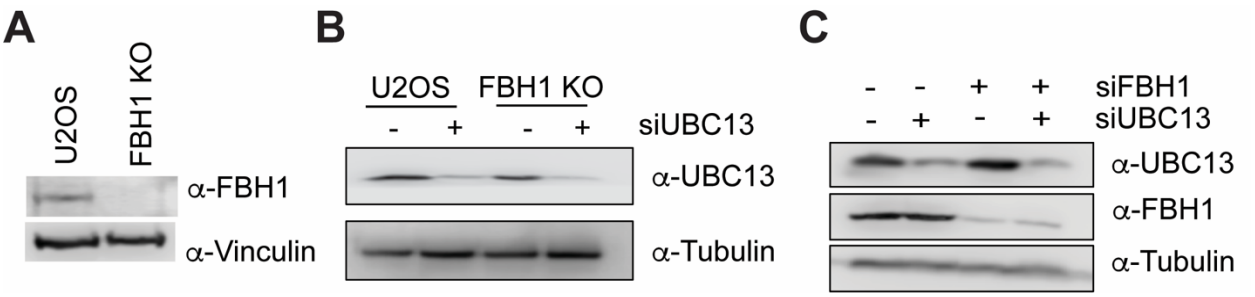

Supplemental Figure 1. FBH1 protein levels in indicated cell lines (A) Western blot showing FBH1 levels in U2OS and FBH1 KO cells. (B) Western blot showing UBC13 knockdown in U2OS and FBH1 KO cells. (C) Western blot showing UBC13 and FBH1 knockdown in RPE-1 cells.

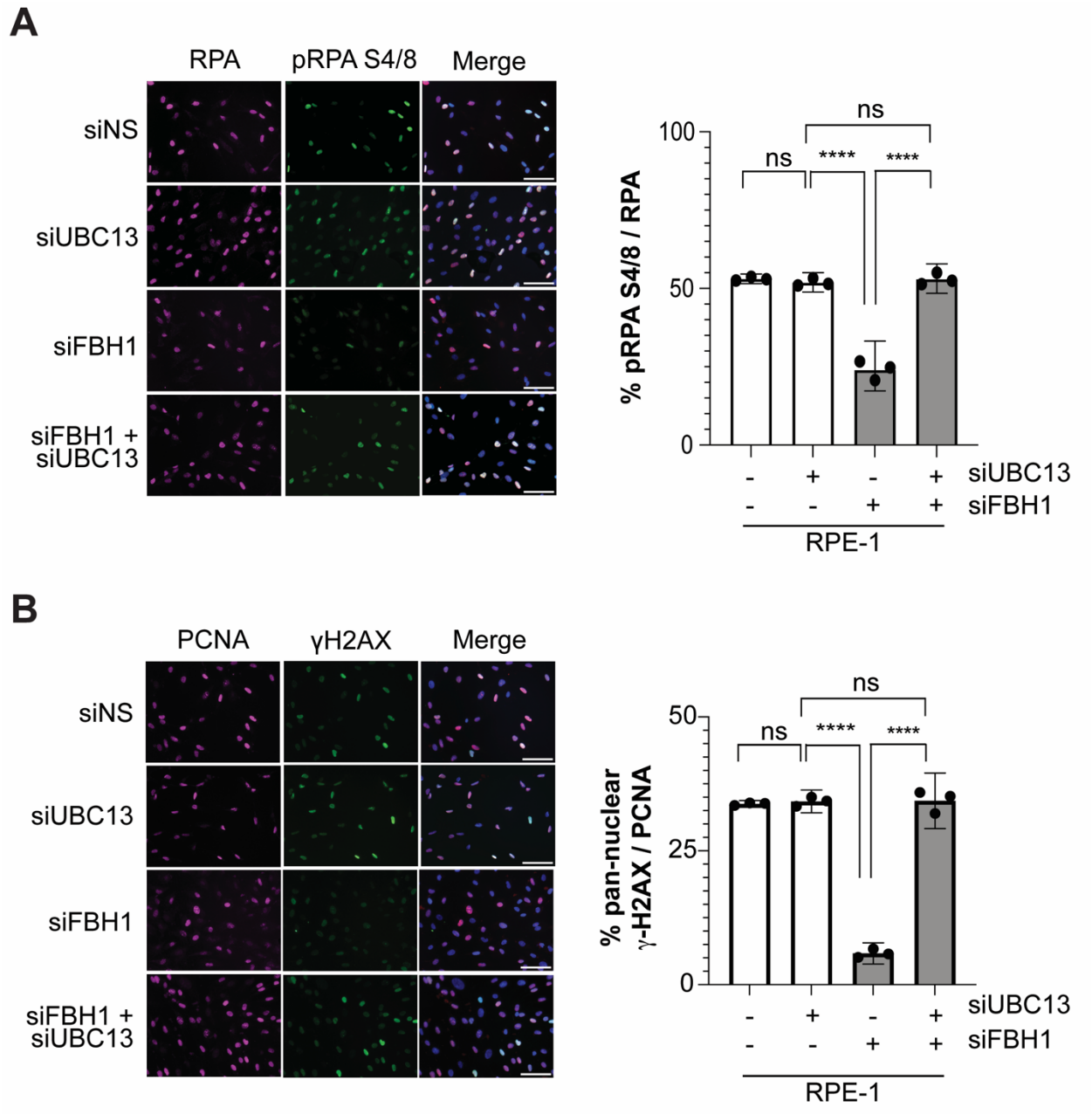

Supplemental Figure 2. Depletion of UBC13 restores DSB signaling in RPE-1 cells. (A) Representative images of pRPA S4/8 (green) and RPA (magenta) in RPE-1 cells treated with 2mM HU after transfection with the indicated siRNAs. DNA is stained with DAPI (blue). Scale bar =100µm. Graph represents mean of three independent experiments. Error bars are standard deviation. **(B)** Representative images of γ-H2AX (green) and PCNA (magenta) in RPE-1 cells treated with 2mM HU after transfection with the indicated siRNAs. DNA is stained with DAPI (blue) Scale bar =100µm. Graph represents mean of three independent experiments. Error bars are standard deviation. ns – not significant. **** - $p<0.0001$. Two-way ANOVA, Tukey.